Measurement of Residual Stress in $YBa_2Cu_3O_{7-x}$ Thin Films by Raman Spectroscopy

Peng Zhao[1] · Xiaoping Ouyang[1] · Jingfeng Yu[2] · Haisheng Xu[2] · Sansheng Wang[3] · Fang Li[3]

Abstract

In this paper, we reported a different approach to measure residual stress state in $YBa_2Cu_3O_{7-x}$ (YBCO) films using Raman spectroscopy. YBCO thin films with the thicknesses of approximately 500 nm were synthesized on $LaAlO_3$ (LAO) and $SrTiO_3$ (STO) substrates using the Trifluoroacetate-organometallic deposition technology (TFA-MOD). A linear relationship was observed between the Raman peak shift and residual stress. Moreover, it was noted that, as for free-standing YBCO and YBCO thin film, a linear relationship was obtained between the Raman peak shift $\Delta\omega$, the residual stress σ, and the stress factor $k = 179.3$ (cm Mpa), i.e., $\sigma = 179.3 \times \Delta\omega\,(Mpa)$. It is found that this method allowed the residual stress of YBCO thin films to be directly measured using the Raman shift factor. This test method can be used for the rapid and non-destructive detection of residual stress in YBCO films.

1 Introduction

Second-generation high-temperature superconductor (HTS)-coated conductors based on films of $REBa_2Cu_3O_{7-\delta}$ (REBCO; RE = Y, Gd, Sm, etc., rare earths) are moving into practical applications for motors, fault current limiters, generators,

---

✉ Peng Zhao
    15673265169@126.com

1   Key Laboratory of Low Dimensional Materials and Application Technology of Ministry of Education, School of Materials Science and Engineering, Xiangtan University, Xiangtan 411105, China

2   Systems Engineering Research Institute, China State Shipbuilding Corporation Limited, Beijing 100094, China

3   Key Laboratory of Micro-nano Measurement, Manipulation and Physics, Ministry of Education, Beihang University, Beijing 100191, China

and transformers [1, 2]. HTS materials have attracted the attention of many researchers accomplish the most promising superconductors available at liquid nitrogen temperature. For practical application, improvements are essential to enhance the current-carrying capacity and superconducting properties of YBCO thin film [3]. However, residual stresses will inevitably be induced in thin films as a result of the structural variation and thermal misfit between the thin film and substrate. The structure and properties of thin films are therefore dependent on residual stress to some degree. Therefore, research into the residual stress in superconducting YBCO thin films is essential.

A large number of theoretical and experimental studies have explored the problem of residual stress, and the experimental determination of residual stress in materials is an integral part of both fundamental and applied research [4]. Scholars have developed many different types of testing techniques, such as X-ray diffraction, Neutron Diffraction Method, Magnetic Method, Ultrasound Method and Indentation Strain Method, but their uses of the occasion are subject to varying degrees of restrictions. For example, the X-ray diffraction method can be used to measure the surface residual stress, the substrate deformation method would destroy the sample [5]. Due to the evolution of X-ray diffraction is difficult in epitaxial orientation and lattice structure, it is hard to accurately measure the residual stress in the composite structures. Therefore, there is an urgent need to develop new testing techniques for micro-scale experimental mechanics, especially for the non-destructive determination of the residual stress in thin films. Raman spectroscopy has unique advantages in the context of non-destructive measurements on the micro-scale, as it is non-destructive and non-contact and has a high spatial resolution (1 μm), broad spectral range, and frequency shift from laser light source frequency limits, with focusing changes can be different depth of the test [6]. In particular, the sensitivity of Raman spectroscopy to the stress in samples of materials in the deformed state causes the Raman spectrum peaks to move and deform, making it possible to measure the mechanical parameters directly [7]. In recent years, Raman spectroscopy combined with mechanical experiments led to applications such as electronic packaging, integrated circuit chips, and micro electromechanical systems [8].

However, to the best of our knowledge, there has been niggardly research on the characterization of residual stresses in YBCO films by Raman spectroscopy up to now. Zeng et al. [9] reported that the influence of the thickness of YBCO thin films on the superconducting transition temperature (T_C) and critical current density (J_C) can be attributed to the variations in interior residual stress and surface morphology associated with the lattice mismatch and grain orientation, respectively. Wang et al. [10] revealed that the roughness and stress were not the main factors that cause the slow or zero increase in J_C. Xiong et al. [11] determined that the values of T_C and J_C were strongly dependent on the film thickness. Following on from these reports, two different substrate structures were used in this study to characterize the residual stress in YBCO films.

The goal of this study was to develop a Raman spectroscopic method for the non-destructive determination of residual stress. A linear relationship was found between the Raman frequency shift and residual stress. The evolution of the residual stress

in YBCO specimens was evaluated using the relationship between the stress and the Raman shift.

2 Experimental Details

2.1 Specimen Preparation

Two kinds of YBCO thin film specimens were prepared on $SrTiO_3$ (YBCO/STO) and $LaAlO_3$ (YBCO/LAO) substrates using the Trifluoroacetate-organometallic deposition technology(TFA-MOD). The preparation process was as follows. Samples of $LaAlO_3(100)$ and $SrTiO_3(100)$ with dimensions of $10 \times 10 \times 1$ mm^3 were selected as substrates. The precursor solution for the deposition of the YBCO films was prepared from yttrium, barium, and copper trifluoroacetates synthesized. The Y, Ba, and Cu sources were mixed in a stoichiometric ratio of 1:2:3. The precursor solution entirely dissolved after several hours of stirring, at which point a stoichiometric amount of trifluoroacetic acid was added into the solution. The precursor solution was then distilled under reduced pressure to obtain a glassy blue residue. This residue was re-dissolved in methanol to a concentration of 1.2 mol/L. The two single-crystal substrates were subjected to different pretreatment processes prior to use owing to their distinct physical properties. The $LaAlO_3$ substrate was ultrasonically cleaned with chloroform, acetone, ethanol, and deionized water (8 min per step) and subsequently dried first with argon gas and then on a hotplate for 10 min. The $SrTiO_3$ substrate was subjected to hydrofluoric acid and two cycles of annealing in air at 1000 °C for 60 min. The precursor solution was then deposited by spin coating at two rotational speeds to give a film thickness of approximately 500 nm.

2.2 Determination of YBCO Thin Films Residual Stress by Raman Spectroscopy

After the object is illuminated by light, there is always a part of light scattering around except reflection, absorption and transmission [12]. Compared with the frequency or wave number of the incident light, the frequency or wave number of scattered light varies greatly [13]. The Raman scattering is when the frequency varies more than 3×10^{10} Hz, and the wave number varies more than 1 cm^{-1} [14]. Raman scattering corresponds to the transition between molecular rotation and vibrational energy levels [15]. Raman spectroscopy can accurately measure the lattice vibration energy of materials. When the material is subjected to stress, the lattice structure will change, the lattice vibration energy will change, and the Raman frequency shift will also change (Raman frequency shift $\Delta \omega$) [16, 17]. According to the relationship between stress and relative Raman frequency shift, the stress in the crystal can be calculated accurately [18].

If stress is present in a specimen, the stress-sensitive Raman bands will move and deform [19]. The frequency shift of the Raman peak is proportional to the stress, as described by Eq. (1):

$$\sigma = k \times \Delta\omega \tag{1}$$

where σ and k are the residual stress and stress factor of the film, respectively, and $\Delta\omega$ is the frequency shift.

Consequently, the type and size of the stress in the film can be measured by the shift in the Raman band. The change in the Raman peak frequency can be simply explained as follows. When compressive stress is applied to a solid, the length of bonds in the molecule typically becomes shorter, and the force constant increases accordingly owing to the relationship between the force constant and bond length, thus increasing the vibrational frequency of the band. Conversely, when the solid is subjected to tensile stress, the band shifts to a lower frequency. Raman spectroscopy is simple to apply and can be used for high-temperature in situ assays. It should be noted that the results of the stress factor k are not uniform in the current measurement of the film stress, so the stress results calculated from the spectral displacement are inconsistent [20]. Therefore, to obtain a more accurate stress value, other thin-film stress measurement methods should be combined with this technique [11].

For simplification, the in-plane surface residual stress in the top coat of YBCO thin film specimens is assumed to be in biaxial plane stress state. Numerous studies have shown that residual compressive stress may cause films to delaminate from their substrates. The first-order Raman spectrum of orthorhombic YBCO presents five Raman active modes, stretching of the apical oxygen (O(4)) along the c-axis, labeled O(4) Ag mode (~500 cm^{-1}) [22]. It has also been shown that the c-axis length presented some ambiguities concerning the oxygen content assessment in thin films [23]. Because of the same method, the same process and three kinds of samples prepared simultaneously, it is considered that the frequency shift of the same O(4) peak of the three samples is mainly caused by the difference of residual stress size and type. Based on the experimental analysis [11], the variety of residual stresses in the film is mainly attributed to oxygen vacancies with thickness of YBCO film increasing. Therefore, when the film thickness was about 500 nm, the frequency shift caused by oxygen content can be neglected compared with that caused by residual stress.

Using the calculated lattice parameters, we can determine the strain in the a axis (ε_a), the b axis (ε_b), and the c axis (ε_c) directly from Eqs. (2)–(4):

$$\varepsilon_a = \frac{a - a_0}{a_0} \tag{2}$$

$$\varepsilon_b = \frac{b - b_0}{b_0} \tag{3}$$

$$\varepsilon_c = \frac{c - c_0}{c_0} \tag{4}$$

where $\varepsilon_a, \varepsilon_b, \varepsilon_c$ are the misfit strains in directions a, b, and c, respectively; a, b, c are the lattice constants of the strained thin film on the substrate; and a_0, b_0, c_0 are the powder sample (unstressed) values ($a_0 = 3.8193$ Å, $b_0 = 3.8847$ Å, and $c_0 = 11.6834$ Å).

The relationship between the three axis system of residual stress in thin films can be applied to the Hook's law isotropic estimate.

$$\varepsilon_a = \frac{1}{E}\left[\sigma_a - \upsilon(\sigma_b + \sigma_c)\right] \tag{5}$$

$$\varepsilon_b = \frac{1}{E}\left[\sigma_b - \upsilon(\sigma_a + \sigma_c)\right] \tag{6}$$

$$\varepsilon_c = \frac{1}{E}\left[\sigma_c - \upsilon(\sigma_a + \sigma_b)\right] \tag{7}$$

For film materials, as the thickness is negligible compared with the substrate and assuming that $\sigma_c = 0$, the in-plane biaxial residual stress of YBCO films can be calculated using Eqs. (8) and (9), which can be deduced from Eqs. (5)–(7):

$$\sigma_a = -\frac{E}{1+\upsilon}\left(\varepsilon_c - \varepsilon_a\right) \tag{8}$$

$$\sigma_b = -\frac{E}{1+\upsilon}\left(\varepsilon_c - \varepsilon_b\right) \tag{9}$$

where E and υ are the elastic modulus and Poisson ratio, respectively (for YBCO, $E = 157$ GPa and $\upsilon = 0.3$ [21]).

Based on the assumption that the YBCO film is an isotropic system, the residual stress in the YBCO film can be expressed as

$$\sigma = \frac{\sigma_a + \sigma_b}{2} \tag{10}$$

3 Results and Discussion

To identify the phase structure and texture of the obtained YBCO films specimens, the specimens were examined by X-ray diffraction (XRD; Philips X'Pert PRO) using filtered Cu Kα radiation at 40 kV and 100 mA. Scanning electron microscopy(SEM; JEOL JSM-5900) was applied to determine the film surface morphology. The Raman spectroscopy characterization has been added to complete the detailed conditions. At room temperature, all the Raman spectra were recorded in a 2 mW power backscattering mode on the 532 nm line of solid-state laser (LabRAMHR Evolution, France). The Raman spectrometer has a resolution of 0.65 cm^{-1}, a measurement range of 200–1000 cm^{-1} and a irradiation time of ∼ 120 s per spectrum. The laser beam is focused on the sample, using a 50X objective lens, and the laser size is 1.25 μm. The critical current density (J_c) was measured using a Jc-scan Leipzig system.

Figure 1a shows the structural model of the YBCO/substrate–film. The thickness of the YBCO film and substrate was approximately 500 nm and 1 mm, respectively.

From RBS analysis, the thickness deviation is less than 10 nm, the compositions ratios of YBCO films are about 1:2:3 or 0.9:2.1:3 in the whole area of YBCO films. The superconducting properties test reveals that with the increase in film thickness of YBCO thin film superconducting properties are not moving in the right direction. Therefore, during film preparation, the thickness of single layer could not be pursued unilaterally, but the thickness of thin film should be pursued with ensuring excellent superconductivity. Through the experiment, when the YBCO film thickness is approximately 500 nm, the optimal critical current density and superconducting transition temperature at the same time. Figure 1b, c presents representative cross-sectional SEM images of the YBCO/LAO and YBCO/STO films, which confirmed that thickness of the films was both merely 500 nm. The cross section of the YBCO/substrate films was found smooth and clearly, and the YBCO film was uniformly covered above the substrate. The films were quite dense.

Figure 2 shows the $\theta/2\theta$ XRD patterns of the YBCO film on the two substrates and the YBCO powder sample. The films were found to grow along the c-axis. According to the result of XRD scanning, it could be calculated according to the software. The detailed steps of the calculation are as follows: first, the XRD diffraction pattern of the sample is obtained by importing the XRD experimental data after calibration on silicon background noise. Then, preliminary phase retrieval is carried out, smoothing the diffraction pattern and removing the object image is further retrieved. Finally, the average lattice constant of grain is calculated. The conventional test could merely give the out-of-plane lattice constant, so other test methods must be found to calculate the in-plane lattice constant of the sample. In this paper, we used the high-resolution asymmetric rocking curve
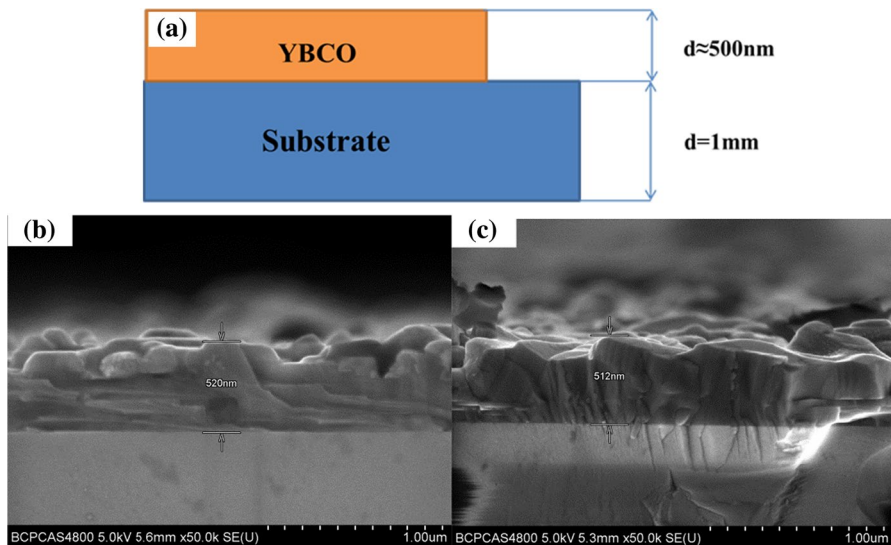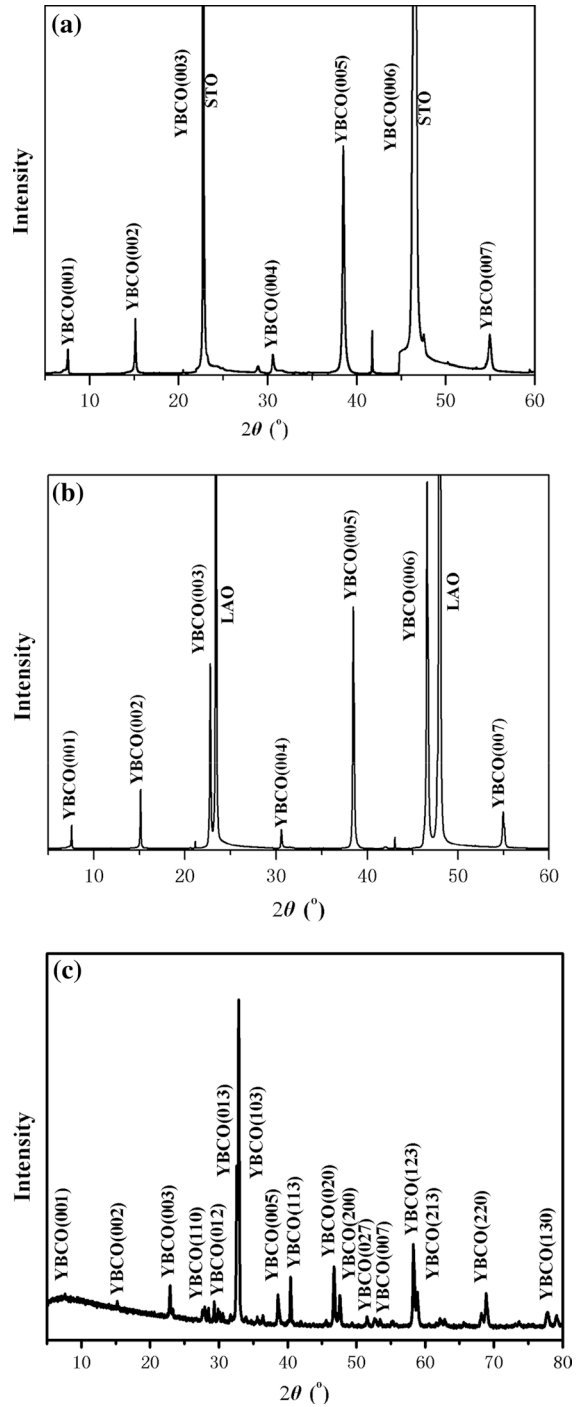

Fig. 1 (Color figure online) **a** Structural model of the YBCO/substrate specimens; typical cross-sectional SEM images of YBCO/substrate films: **b** YBCO/STO (film thickness: 520 nm), **c** YBCO/LAO (film thickness: 512 nm)

Fig. 2 $\theta/2\theta$ XRD patterns of the YBCO epitaxial films on the two substrates and the YBCO powder sample: **a** YBCO/STO, **b** YBCO/LAO, **c** YBCO powder sample

to test the out-of-plane and the in-plane lattice constant of the YBCO film sample. Through the high-resolution diffraction pattern, we can calculate the c-axis lattice constant of the YBCO film. The in-plane lattice constant usually selects a specific asymmetric surface (hkl), which was calculated by the interplanar spacing and the angle between the faces, and the YBCO belongs to the orthorhombic system.

In this experiment, the [103] of the LAO substrate and the [109] faces of YBCO were used to calculate the a-axis length of the YBCO film. The b-axis length of the YBCO film can be obtained by testing the [013] face of the LAO substrate and the [019] face of the YBCO film. Similarly, [103] planes of STO substrate and [109] planes of YBCO were used to calculate the a-axis length of YBCO films. The b-axis length of YBCO thin films can be obtained by measuring the [013] surface of STO substrate and the [019] surface of YBCO thin films. XRD was also carried out to evaluate the residual stress distribution in the YBCO specimens, to confirm the reliability of the results obtained from the Raman measurements. Both films were found to be single phased and grow in a (00 l) orientation normal to the substrate surface. No other orientation of YBCO was detected, indicating good-quality films with c-axis orientation.

Figure 3 shows the Raman spectra of the YBCO powder sample, YBCO/LAO sample, and YBCO/STO sample. Figure 4 shows Raman shifts of the O4 phonon mode for the YBCO power sample(a), YBCO/LAO(b), and YBCO/STO(c), and the corresponding Raman shifts of the phonon peak lattice information associated with the O4 phonon mode. Raman spectroscopy is a commonly tool for studying the microstructure of molecular systems, especially for analyzing the relationship between superconductivity and structure of YBCO films. Based on the lattice parameters ($a = 3.8012$ Å, $b = 3.8534$ Å, $c = 11.7312$ Å), the residual stress in the YBCO film was calculated by using Eqs. (1–10). Take YBCO/LAO sample
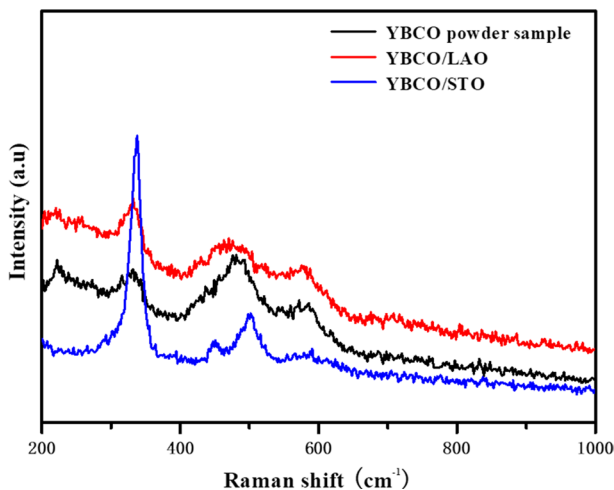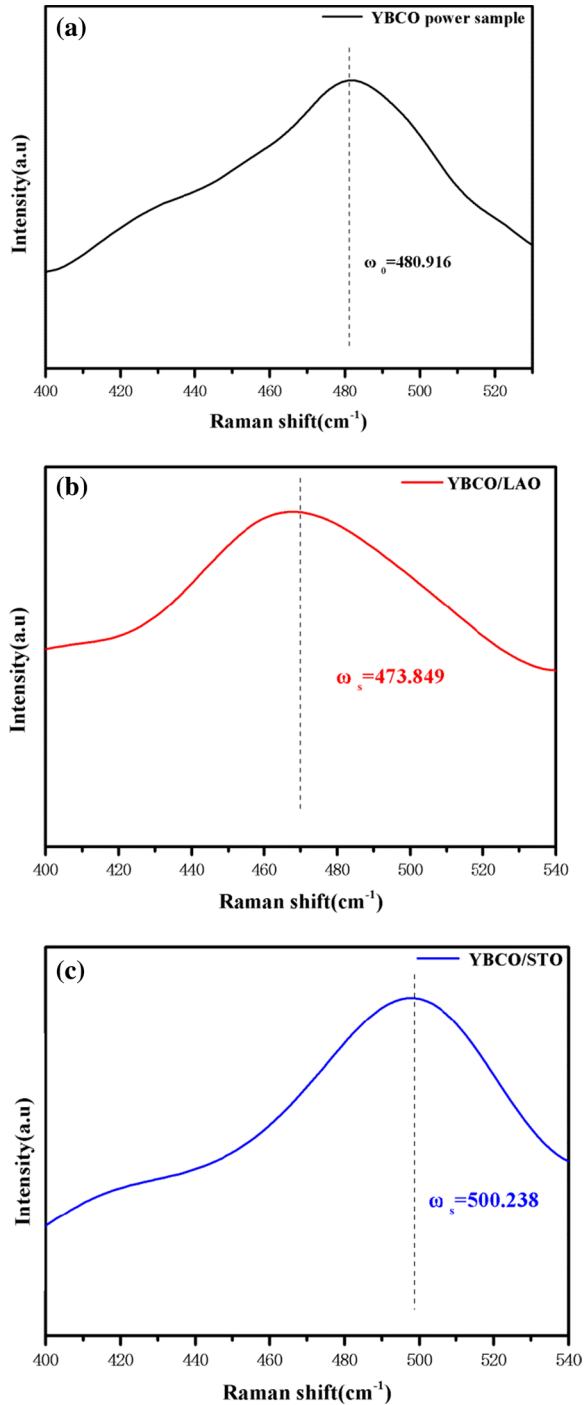

Fig. 3 (Color figure online) Typical Raman spectra of the YBCO powder sample, YBCO/LAO, and YBCO/STO

Fig. 4 (Color figure online) Raman shifts of the phonon peak lattice information associated with the O4 phonon mode for the YBCO power sample (**a**), YBCO/LAO (**b**), and YBCO/STO (**c**)

for example, we can determine the strain in the a axis (ε_a), the b axis (ε_b) and the c axis (ε_c) directly from Eqs. (2)–(4):

from Eqs. (2), we can get ε_a,

$$\varepsilon_a = \frac{a - a_0}{a_0} = \frac{3.8012 - 3.8193}{3.8193} = -0.0047$$

from Eqs. (3), we can get ε_b,

$$\varepsilon_b = \frac{b - b_0}{b_0} = \frac{3.8534 - 3.8847}{3.8847} = -0.00806$$

from Eqs. (4), we can get ε_c,

$$\varepsilon_c = \frac{c - c_0}{c_0} = \frac{11.7312 - 11.6834}{11.6834} = -0.00409$$

The relationship between the three axis systems of residual stress in thin films can be applied to the Hook's law isotropic estimate, from Eqs. (5)–(7), we can get Eq. (8)

$$\sigma_a = -\frac{E}{1 + \upsilon}\left(\varepsilon_c - \varepsilon_a\right) = -\frac{157}{1 + 0.3}(0.00409 + 0.0047) = -1062 \, \text{MPa}$$

from Eqs. (5)–(7), we can get Eq. (9)

$$\sigma_b = -\frac{E}{1 + \upsilon}\left(\varepsilon_c - \varepsilon_b\right) = -\frac{157}{1 + 0.3}(0.00409 + 0.00806) = -1468 \, \text{MPa}$$

from Eqs. (5)–(7), we can get Eq. (10)

$$\sigma_{\text{YBCO/LAO}} = \frac{\sigma_a + \sigma_b}{2} = \frac{-1062 - 1468}{2} = -1265 \, \text{MPa}$$

According to the above calculation steps, we can also calculate the residual stress of YBCO/STO samples.

$$\sigma_{\text{YBCO/STO}} = 3457 \, \text{MPa}$$

Take YBCO/LAO sample for example, from Eq. (1) $\sigma = k \times \Delta\omega$, we can get the k_1,

$$k_1 = \frac{\sigma_{\text{YBCO/LAO}}}{\Delta\omega} = \frac{-1265}{-7.037} = 179.7 \, (\text{cm MPa})$$

When the YBCO/STO sample, from Eq. (1) $\sigma = k \times \Delta\omega$, we can also get the k_2,

$$k_2 = \frac{\sigma_{\text{YBCO/STO}}}{\Delta\omega} = \frac{3457}{19.322} = 178.9 \, (\text{cm MPa})$$

For the accuracy of the test results, we take an average value:

$$k = \frac{k_1 + k_2}{2} = \frac{179.7 + 178.9}{2} = 179.3 \text{ (cm MPa)}$$

The result is also within a reasonable error range.

The residual stress was -1265 MPa, where $\Delta\omega = \omega_s - \omega_0$, ω_s and ω_0 are the peak position of the stressed state and the peak position of the stress-free state, respectively. From the results shown in Fig. 5a–c, the frequency shift $\Delta\omega$ between the YBCO/LAO film and the YBCO powder sample was calculated to be -7.037. The stress factor was 179.7. As shown in Tables 1 and 2, the residual stress of the YBCO/STO film was 3457 MPa, which is consistent with the results of the previous investigations [11].

The SEM images shown in Fig. 5 reveal the surface morphologies of the YBCO films on the two substrates. From Fig. 5a, a lot of needle-like grains can be seen in YBCO/LAO film, and these grains are generally considered as a-axis grain growth [23], and the thin films grow densely with fewer pores. The appearance of a-axis grains will cause tensile stress in the upper layer of the superconducting film [24]. The existence of pores is conducive to the release of residual stress in the film [25]. The pores formed on the surface of YBCO thin film make the film less dense and
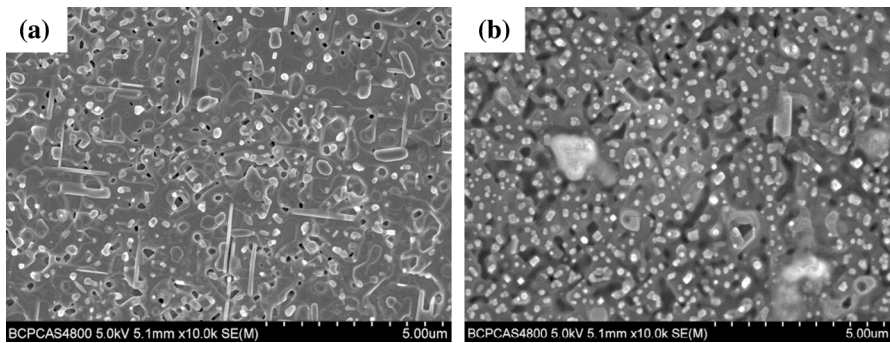

Fig. 5 SEM images showing the surface morphologies of the films: **a** YBCO/STO, **b** YBCO/LAO

Table 1 Frequency shifts of the different specimens

Specimen	ω_0	ω_S	$\Delta\omega$
YBCO powder sample	480.916	–	–
YBCO/LAO	–	473.879	-7.037
YBCO/STO	–	500.238	19.322

Table 2 Lattice parameters, strain, and residual stress calculated from XRD

Specimen	a (Å)	b (Å)	c s(Å)	ε_a	ε_b	ε_c	σ(MPa)
YBCO powder sample	3.8193	3.8847	11.6834	–	–	–	–
YBCO/LAO	3.8012	3.8534	11.7312	-4.7×10^{-3}	-8.1×10^{-3}	4.1×10^{-3}	-1265
YBCO/STO	3.8243	3.6503	11.6750	1.3×10^{-3}	-6.0×10^{-2}	-7.2×10^{-4}	3457

then affect the superconductivity of the thin film. From Fig. 5b, it can be seen that more pores was produced in the YBCO/STO film, which is useful for the residual stress released. This discussion is consistent with the results calculated in Table 2.

Figure 6 shows the values of the superconducting critical current density J_C for the YBCO films on the two substrates. Due to the existence of pores, the in-plane residual stress in the YBCO thin film is diminished, which result from the higher J_C in YBCO/LAO sample. In addition, we found that the larger residual stress in the film leads to the smaller J_C. Then, we deduced that the residual stress of the YBCO superconducting film has a certain inhibition on J_C. It is found that the existence of large tensile stress will lead to the formation of a-axis grain growth and the loss of superconductivity [25], resulting in the decrease of J_C, which corresponds to the results of X-ray diffraction and SEM images.

Figure 7 shows the superconducting transition temperature T_c distribution of YBCO thin films on the two substrates. From Fig. 7a, b, it is clear that the superconducting transition temperature of the YBCO film on the STO substrate is higher than the superconducting transition temperature of the YBCO superconducting film on the LAO substrate, but the difference is not big.

4 Conclusions

A different approach was applied to measure residual stress state in YBCO films using Raman spectroscopy. YBCO thin films with the thicknesses of approximately 500 nm were synthesized on LAO and STO substrates using the TFA-MOD. Residual stress state in YBCO specimens was determined using the Raman shift. A linear relationship was observed between the Raman peak shift and residual stress. Moreover, it is noted that, as for free-standing YBCO and YBCO thin film, a linear relationship was obtained between the Raman peak shift $\Delta\omega$, the residual stress σ, and the stress factor $k = 179.3$ (cm Mpa), i.e.,
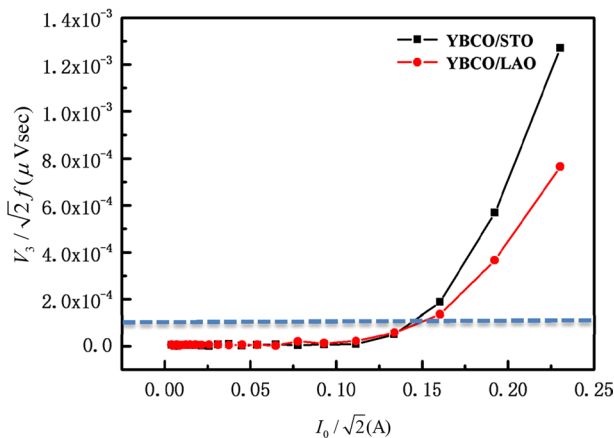

Fig. 6 (Color figure online) J_c profiles for the superconducting YBCO thin films
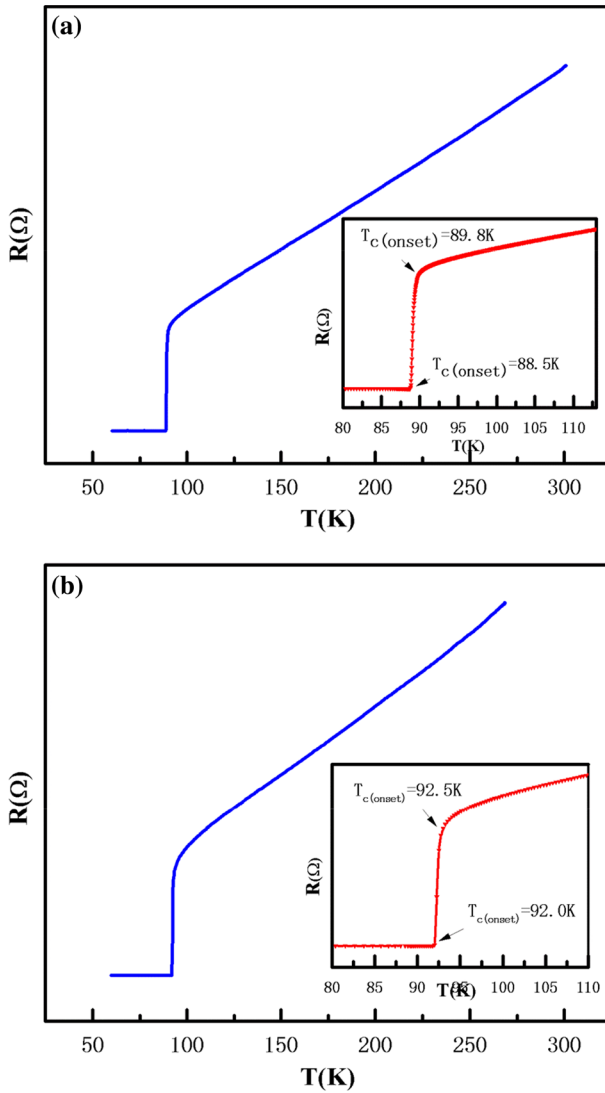
Fig. 7 (Color figure online) T_c profiles for the superconducting YBCO thin films: **a** YBCO/LAO, **b** YBCO/STO

$\sigma = 179.3 \times \Delta\omega\,(Mpa)$. It is found that this method allows the residual stress of YBCO thin films to be directly measured using the Raman shift factor.

References

1. D. Larbalestier, A. Gurevich, D.M. Feldmann, A. Polyanskii, High-T_c superconducting materials for electric power applications. Nature **414**(6861), 368–377 (2001)
2. A.B. Abrahamsen, N. Mijatovic, E. Seiler, T. Zirngibl, C. Træholt, P.B. Nørgård et al., Superconducting wind turbine generators. Supercond. Sci. Technol. **23**(3), 034019 (2010)
3. G. Kaltsas, A.G. Nassiopoulou, M. Siakavellas, E. Anastassakis, Stress effect on suspended polycrystalline silicon membranes fabricated by micromachining of porous silicon. Sens. Actuators A Phys. **68**(1), 429–434 (2015)
4. I.D. Wolf, Micro-raman spectroscopy to study local mechanical stress in silicon integrated circuits. Semicond. Sci. Technol. **11**(2), 139 (1999)
5. E. Anastassakis, A. Cantarero, M. Cardona, Piezo-raman measurements and anharmonic parameters in silicon and diamond. Phys. Rev. B Condens. Matter **41**(11), 7529 (1990)
6. Z. Lei, Y. Kang, M. Hu, Y. Qiu, H. Xu, H. Niu, An experimental analysis of residual stress measurements in porous silicon using micro-Raman spectroscopy. Chin. Phys. Lett. **21**(2), 403–405 (2004)
7. I.D. Wolf, Stress measurements in si microelectronics devices using Raman spectroscopy. J. Raman Spectrosc. **30**(10), 877–883 (1999)
8. K. Suzuki, T. Araki, T. Konno, T. Suzuki, I. Hirabayashi, Y. Enomoto, Microwave characteristics and Jc, distribution of TFA-MOD YBCO film. Phys. C Supercond. Appl. **372–376**(12), 623–625 (2002)
9. L. Zeng, Y.M. Lu, Z.Y. Liu, C.Z. Chen, B. Gao, C.B. Cai, Surface texture and interior residual stress variation induced by thickness of $YBa_2Cu_3O_7$-δ thin films. J. Appl. Phys. **112**(5), 189 (2012)
10. Y. Wang, D. Xu, Y. Li, L. Liu, Dependencies of microstructure and stress on the thickness of $GdBa_2Cu_3O_7$-δ thin films fabricated by rf sputtering. Nanoscale Res. Lett. **8**(1), 304 (2013)
11. J. Xiong, W. Qin, X. Cui, B. Tao, J. Tang, Y. Li, Thickness-induced residual stresses in textured YBCO thin films determined by crystalline group method. Phys. C Supercond. Appl. **455**(1–2), 52–57 (2007)
12. M. Becker, G. Sarau, H.P. Strunk, S. Christiansen, *Raman Imaging of Grain Orientation, Strain, Crystallinity and Doping Levels in Solar Silicon. Raman Imaging*, vol. 168 (Springer, Berlin, 2012), pp. 257–299
13. Z. Wu, J. Zhou, W. Chen, J. Shen, C. Lv, Effects of residual stress on the electrical properties in $PbZr_{0.52}Ti_{0.48}O_3$, thin films. J. Sol-Gel Sci. Technol. **75**(3), 1–6 (2015)
14. H. Miyagawa, D. Kamiya, C. Sato, K. Ikegami, Strain measurement for Raman-inactive substrates with pbo thin films using raman coating method. J. Mater. Sci. **34**(1), 105–110 (1999)
15. J.L. Fang, Y. Wu, The principle and application of surface enhanced Raman spectroscopy (SERS) (in Chinese). Surf. Technol. **23**(4), 167–173 (1994)
16. M. Qiu, W.G. Mao, C.Y. Dai, Y.C. Zhou, Micro-Raman spectroscopy technique applications to measure stress fields in thermal barrier coatings (in Chinese). J. Changsha Commun. Univ. **22**(2), 76–80 (2006)
17. P. Jannotti, G. Subhash, Measurement of residual stresses in B4C–SiC–Si Ceramics Using Raman Spectroscopy, in *Conference on Experimental and Applied Mechanics* (2016)
18. H.D. Wagner, M.S. Amer, L.S. Schadler, Residual compression stress profile in high-modulus carbon fiber embedded in isotactic polypropylene by micro-Raman spectroscopy. Appl. Compos. Mater. **7**(4), 209–217 (2000)
19. T. Tomimatsu, Y. Kagawa, S.J. Zhu, Residual stress distribution in electron beam-physical vapor deposited ZrO_2, thermal barrier coating layer by Raman spectroscopy. Metall. Mater. Trans. A **34**(8), 1739–1741 (2003)
20. W. Feng, N. Watanabe, H. Shimamoto, M. Aoyagi, K. Kikuchi, Residual stress investigation of via-last through-silicon via by polarized Raman spectroscopy measurement and finite element simulation. Jpn. J. Appl. Phys. **57**, 07MF02 (2018)
21. J.H. Cheon, P.S. Shankar, J.P. Singh, Influence of processing methods on residual stress evolution in coated conductors. Supercond. Sci. Technol. **18**(1), 142 (2005)
22. S. Degoy, J. Jiménez, P. Martin, O. Martinez, A.C. Prieto, D. Chambonnet et al., Oxygen content of YBaCuO thin films. Phys. C Supercond. **256**(3), 291–297 (1996)

23. P.C. Mcintyre, M.J. Cima, F.N. Man, Metalorganic deposition of high-Jc $Ba_2YCu_3O_{7-x}$ thin films from trifluoroacetate precursors onto (100) $SrTiO_3$. J. Appl. Phys. **68**(8), 4183–4187 (1990)
24. Y. Yeshurun, A.P. Malozemoff, Giant flux creep and irreversibility in an Y–Ba–Cu–O crystal: an alternative to the superconducting-glass model. Phys. Rev. Lett. **60**(21), 2202–2205 (1988)
25. J. Xiong, W. Qin, X. Cui et al., High-resolution XRD study of stress-modulated YBCO films with various thicknesses. J. Cryst. Growth **300**(2), 364–367 (2007)